Failure Mechanism of Sandwich Panels Under Three-Point Bending

Raja Ouled Ahmed Ben Ali(✉) and Sami Chatti

LMS, Ecole Nationale d'Ingénieurs de Sousse, Sousse, Tunisie
ouledahmed_raja@live.fr, sami.chatti@enim.rnu.tn

Abstract. Sandwich materials are potential candidates instead of traditional materials in several fields as aerospace, civil engineering and automotive because of their mechanical properties and especially their high ratio bending stiffness to weight. Three-point bending is a frequent process for forming sandwich panels before usage. This study presents an analysis of the damage of the sandwich panels during quasi-static tests in three-point bending. Experimental tests leading to the failure of the core of the sandwich material were carried out. Finite element analysis was also conducted for the numerical prediction of observed damage. Also, analytical Gibson's modified model is considered to obtain the critical loads leading to the failure of the sandwich panels. This allows constructing a mode map for failure modes of sandwich panels in three points bending process.

Keywords: Three points bending · Thick sandwich panel · Numerical simulation · Damages · Failure map

1 Introduction

Sandwich plates are increasingly used in a wide range of industrial products [1] varying from automobiles and airplanes to simple home appliances due to the properties such as lightweight, vibration reduction, acoustic noise damping, and heat insulation [2]. In addition, the sandwich panel metal/polymer/metal have been tested in standard or specialized tests such as shearing, three point bending, four point bending, and indentation [3–5]. The most common failure mode of the foam core sandwich structures is core shearing, followed by local indentation collapse and face yielding [3, 5, 6]. The risk of mechanical buckling, and decohesion between the skins and the core constitute the main weaknesses of sandwich panels. Under bending, a sandwich panel undergoes various modes of degradation classified in several categories by [7–9]. Kim and Hwang [10] studied theoretically and experimentally the effect of decohesion between skin and core on the stiffness of sandwich panels. Idriss et al. [11] have shown that the crack propagation occurs in three stages: decohesion between the core and the upper skin, core shear and debonding between the lower skin and the core. However, among these studies, there is a lack of systematical research on the steel/polyurethane/steel sandwich structures' failure mechanism. Based on the aforementioned literature, limited study was conducted on the modeling of damage propagation in polyurethane foam cores. For the above-mentioned reasons, in this paper the

N. Aifaoui et al. (Eds.): CMSM 2019, LNME, pp. 533–544, 2020.
https://doi.org/10.1007/978-3-030-27146-6_58

failure mechanism of sandwich panel in three point bending test are investigated by applying the cellular solids theory [12]. In addition, experiments and numerical simulations are carried out to validate the theoretical prediction.

2 Analytical Analysis

Several failure modes have been identified for sandwich panels in three-point bending [12]: (a) face yielding; (b) wrinkling of the compressive face; (c) core shearing, (d) face debonding, (e) indentation. The last mode of failure occurs when the loading is extremely localized and can be avoided by increasing the loading area. To analyze the failure mechanism of the panels, it is necessary to characterize the normal stress and the shear stress acting on the skins and the core.

The maximum stress occurs in the cross section which has the maximum moment. In the load case of three-point bending, the maximum moment and the shear can be easily acquired in terms of the concentrated load P, that:

$$M = \frac{PL}{4} \tag{1}$$

Considering the shear stress as linear through the faces and constant through the core since the faces are much stiffer and thinner than the core, the normal and shear stresses can be expressed as [13]:

$$\sigma_{p\max} = \pm \frac{PL}{4e_p bd} \tag{2}$$

$$\sigma_{c\max} = \pm \frac{PLe_c}{8D} E_c \tag{3}$$

$$\tau_{c\max} = \frac{P}{2bd} \tag{4}$$

where D is the equivalent flexural rigidity, which can be expressed as [13]:

$$D = \frac{E_p e_p d^2 b}{2} + \frac{E_p t_p^3 b}{6} + \frac{E_c e_c^3 b}{12} \tag{5}$$

2.1 Modified Gibson's Model

Instead of a flat loading head and supports used in the experiments and analysis of [3], a cylindrical loading head and supports are used in the present experiments and analysis. Hence some modifications are required. Three main failure modes of sandwich panel steel/polyurethane/steel (face yielding, wrinkling face and core shearing) are considered in this study.

Face yielding

This mode occurs when the maximum normal stress in faces reaches the yield strength of the face material

$$\sigma_p = \sigma_{yp} \tag{6}$$

where

σ_{yp}: yield strength of the face material

The critical load for the face yield mode is given by

$$P_{cr1} = \frac{4be_pe_c}{L}\sigma_{yp} \tag{7}$$

Wrinkling face

This mode occurs when the maximum normal stress in faces reaches the local elastic instability stress, in this case:

$$\sigma_p = \sigma_{wp} \tag{8}$$

σ_{wp} is wrinkling stress in the face material which can be expressed as follow [13]:

$$\sigma_{wp} = \frac{3E_p^{1/3}E_c^{2/3}}{\left[12(3-\upsilon_c)^2(1+\upsilon_c)^2\right]^{1/3}} \tag{9}$$

where υc: Poisson's ratio of foam material

The critical load of wrinkling face mode is given as [14]:

$$P_{cr2} = \frac{4be_pe_c}{L}E_p^{1/3}E_s^{2/3}\left[0.28\left(\frac{\rho_c}{\rho_s}\right)^{4/3} + 0.2\left(\frac{\rho_c}{\rho_s}\right)^{2/3}\right] \tag{10}$$

where ρ_s, E_s: Density and Young's modulus of foam's cell-wall material, respectively.

Core shearing

The shear force is carried mainly by the foam core when the sandwich panel is subjected to a transverse shear force. If the shear stress in the foam core reaches the shear strength of the foam core material, the initial failure will be in the foam core. The critical load of core shear mode is written as [14]:

$$P_{cr3} = 2be_c\left[2.32\left(\frac{\rho_c}{\rho_s}\right)^{3/2} - 0.28\frac{\rho_c}{\rho_s}\right]\sigma_{ys} \tag{11}$$

where σ_{ys} Yield strength of foam's cell-wall material

Table 1 gives the mechanical and geometrical characteristics of sandwich panels Steel/Polyurethane/Steel (Table 1).

Table 1 Mechanical and geometrical characteristics of sandwich panels Steel/Polyurethane/Steel

Panel's geometry (mm)			Skin material (MPa)		Core material (Kg/m^{3}MPa)			
b	e_p	e_c	E_p	σ_{yp}	ρ_c	ρ_s	E_s	σ_{ys}
50	0.5	40	200000	400	40	1170	1600	53.4

Figure 1 plots the sandwich panel failure loads of different failure modes in terms of the length between supports L. From this figure it is observed that the critical loads of the first two failure modes decrease with increasing length between the supports L, while the critical load of the shear failure of the core is constant. In addition, it is observed that the panels suffer a failure according to the mode of core shear for lengths between weak supports. While, for wide distances between supports, it is the folding mode of the skins which intervenes. In addition, the skin yielding failure mode is less likely to occur since the corresponding failure limit load is much higher than the other two modes.

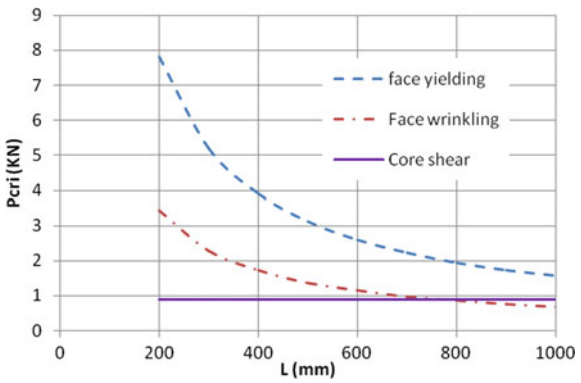

Fig. 1 Failure loads of sandwich panel steel/polyurethane/steel

2.2 Failure Mode Map

The failure mode map can be constructed from Eqs. (7) (10) and (11), with dimensionless parameters the relative density of foam ρc/ρs and ratio of skin thickness to span length ep/L as the coordinates. The diagram is divided into three regions. Within each region one failure mechanism is dominant. The regions are separated by three transition lines, which represent the panel designs for which two mechanisms have the same failure load. The three transition lines are governed by Eqs. (12), (13) and (14), respectively, skin folding and skin lamination, skin wrinkling and core shear and that between core shear and plasticization of skin. These equations are obtained for equal critical loads for two particular failure modes. It is clear that these transition lines depend mainly on the strength of face and core materials.

$$\frac{\rho_c}{\rho_s} = \left(\frac{\sigma_{yp}}{0.26\, E_p^{1/3}\, E_S^{2/3}} \right)^{3/2} \tag{12}$$

$$\frac{\rho_c}{\rho_s} = \left(\frac{0.85 ep E_p^{1/3}\, E_s^{2/3}}{0.62\, \sigma_s L} \right)^{4} \tag{13}$$

$$\frac{\rho_c}{\rho_s} = \left(\frac{1.13 \sigma_p e_p}{0.65\, \sigma_s L} \right)^{3/4} \tag{14}$$

An initial failure mode map according to the geometry and material properties of sandwich panels steel/polyurethane/steel is predicted in Fig. 2.

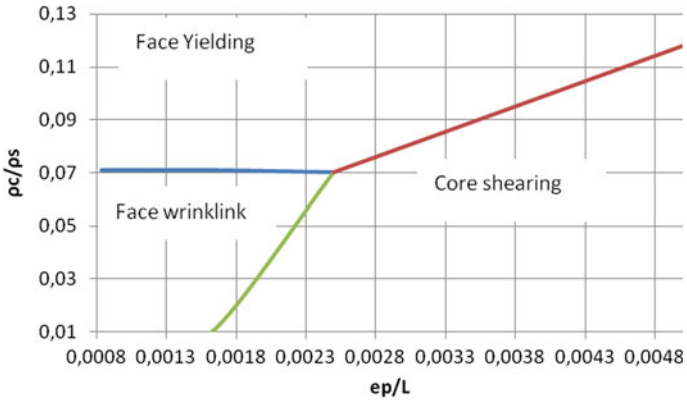

Fig. 2 Failure mode map of sandwich panel steel/polyurethane/steel

3 Experimental and Numerical Procedures

3.1 Experimental Procedures

The core of the sandwich specimens used in this study consists of polyurethane PUR is closed-cell rigid foam plastic. The foam properties could be obtained from uniaxial compression tests according to ASTM C 365-57 standard. The skin used in this study consists of galvanized steel with high specific strength and stiffness. The skin properties could be obtained from tensile tests according to NF EN 10002-1 standard. The mechanical properties of the polyurethane foam core and the steel skin were experimentally obtained and reported in Table 2.

Table 2 Mechanical properties of the steel skin and the polyurethane foam core

	Steel skins	Foam core
Density ρ [kg/m^3]	7800	40
Yield stress σ_0 [MPa]	440	0.41
Young's modulus E [MPa]	200000	3.31
Poisson's ratio ν	0.3	0.4
Strength R_m [MPa]	453	0.53

Quasi-Static three-point bending tests were conducted with the MTS testing machine to acquire the load–displacement curves (Fig. 3). All the specimens were obtained from sandwich panels composed by a polyurethane foam core and steel skins. Subsequent tests are performed with a displacement rate of 10 mm/min. The specimens were tested to failure.

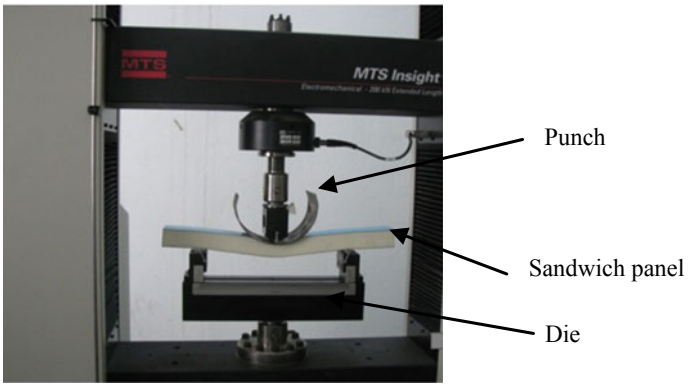

Fig. 3 Experimental set-up of the three-point bending test

3.2 Numerical Simulations

The FEM software package ABAQUS/Explicit was used to simulate the three-point bending of sandwich sheets. Figure 4 gives the two-dimensional geometric modeling with Abaqus software with a mesh size sufficiently refined to ensure precise results and adequate boundary conditions. Due to the material symmetry, only a half of the section of the sandwich panel was considered. The core was modeled as foam of an elastic–plastic material using hardening curves obtained from compression tests. The skin sheet was modeled as elastic-plastic material.

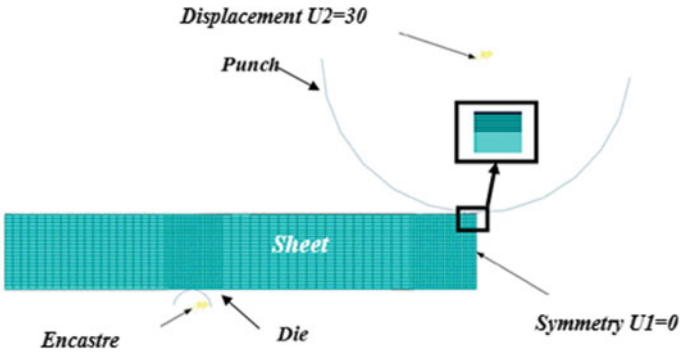

Fig. 4 FE model of three-point bending process

Damage initiation in the foam core was modeled by a shear damage criterion.

The shear criterion assumes that the equivalent plastic strain at the onset of the damage. $\bar{\varepsilon}_S^{pl}$ is a function of the shear ratio and strain rate:

$$\bar{\varepsilon}_S^{pl}\left(\theta_S, \dot{\bar{\varepsilon}}^{pl}\right) \tag{15}$$

where $\theta_S = (q + k_s p)/\tau_{max}$ is the shear stress ratio, τ_{max} is the maximum shear stress, and k_s is a material parameter. The damage onset is occurred when:

$$w_S = \int \frac{d\bar{\varepsilon}^{pl}}{\bar{\varepsilon}_S^{pl}\left(\theta_S, \dot{\bar{\varepsilon}}^{pl}\right)} = 1 \tag{16}$$

where ω_S is a state variable which increases with the equivalent plastic strain.

4 Results and Discussion

Figure 5a shows a shear failure of the core in three-point bending. Since foams have generally lower mechanical properties than skins, they will be affected by damage initiation. Figure 5b shows another mode of fracture: debonding skin/core that spreads

under the skin several millimeters along the length of the panel. This fracture is due to the presence of defects in the junction between the skins and the foam.

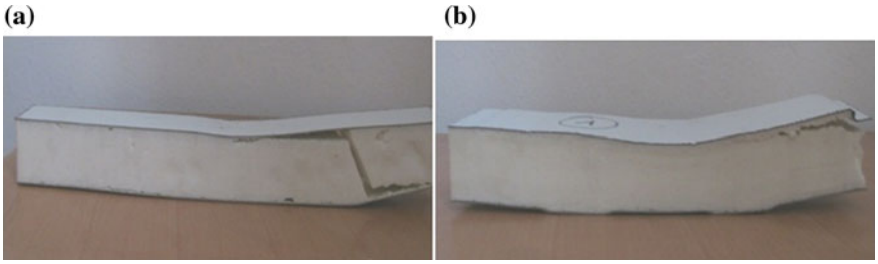

Fig. 5 Failure modes of sandwich panels, **a** Shear failure of the core; **b** debonding skin/core

Figure 6 shows the curves of the stored energies ALLKE, ALLIE and ALLKE/ALLIE versus time. This figure shows that the kinetic energy (ALLKE) does not exceed 5% of the total energy (ALLIE), which demonstrates that the influence of inertial force is within the acceptable range.

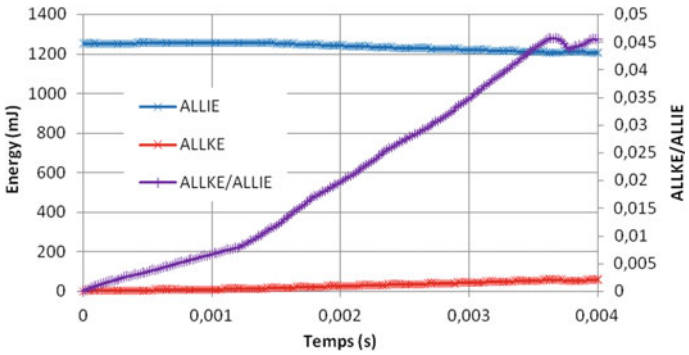

Fig. 6 ALLKE, ALLIE and ALLKE/ALLIE ratio versus time curves

Figures 7 and 8 show experimental and numerical load-displacement curves of sandwich panel in three-point bending test. The obtained curves can be divided into three regions. In the first region, a linear trend is observed with a small deformation. The second region corresponds to a nonlinear behavior in which the maximum load is reached, significant drop of the peak load is observed for all sandwich structures. This sudden drop is due to the foam cracking. In the third region, a plateau was observed until failure with small evolution and the specimen continued to sustain the load but never exceeded the previous peak load. It can be seen that a satisfactory agreement was found between the experimental result and the FEA result. The peak load in numerical results was slightly higher than the experimental ones. This is due to initial defects in sandwich composite which is not considered in FEM analysis. Figure 7 plots the

load-displacement curves by considering the effect of the distance between supports. From this figure it can be seen that the failure parameters (loads and displacements) increase with the decrease of the distance between supports as can be expected. Figure 8 shows that the failure parameters increase with the increase of the foam thickness. Values of failure loads, failure displacements and stiffness are presented in Tables 3 and 4.

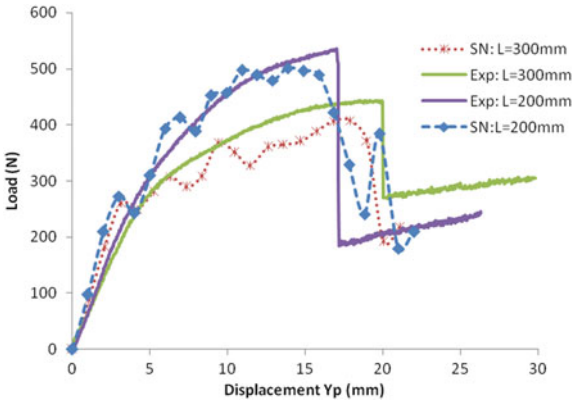

Fig. 7 Bending curves for different lengths between supports

Table 3 Static characteristics of sandwich panel for different length between supports

	L = 200 mm	L = 300 mm
Failure load (N)	514	411
Failure displacement (mm)	17.7	19.3
Stiffness (N/mm)	82	61

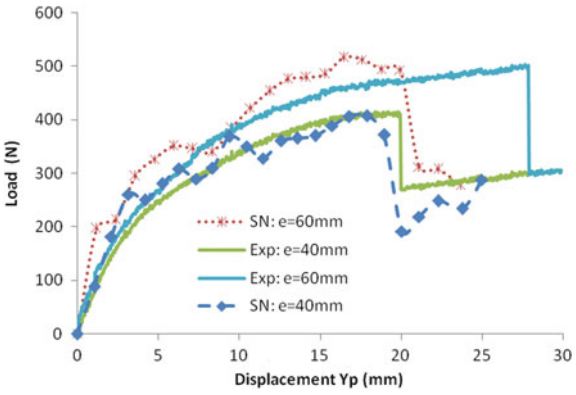

Fig. 8 Bending curves for different foam thickness

Total equivalent plastic strain occurred in the sandwich plates are gathered from the finite elements analyses and illustrated in Fig. 9. As can be seen, the maximum equivalent plastic strain is located in the foam under the punch and in the lower part of the foam inclined at about 45° to the punch/panel contact. Notice that failure was initiated at these locations.

Table 4 Static characteristics of sandwich panel for different foam thickness

	e = 40 mm	e = 60 mm
Failure load (N)	411	476
Failure displacement (mm)	19.3	22.2
Stiffness (N/mm)	61	73

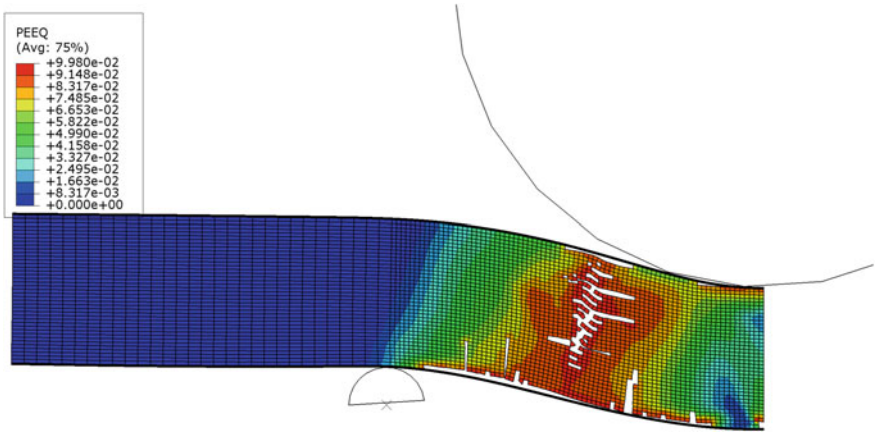

Fig. 9 Equivalent plastic strain distribution

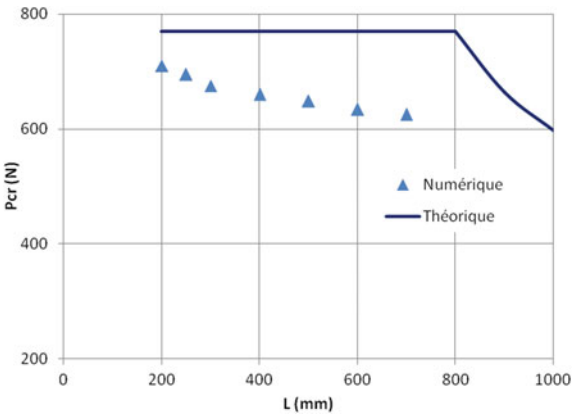

Fig. 10 Numerical results of the failure loads of the sandwich panel steel/polyurethane/steel

Figure 10 gives a comparison between the critical loads obtained from the theoretical studies, concerning the two modes of damage skin wrinkling and core shearing, and the loads obtained numerically. From this figure we observe that the maximum error is 21% which can be explained by the simplifying assumptions used in obtaining the theoretical failure criteria.

5 Conclusion

The purpose of this paper is to investigate the damage behavior of sandwich panel steel/polyurethane/steel by considering the effect of the variation of several geometrical parameters during quasi-static tests in three-point bending. Experimental tests leading to the failure of the core of the sandwich material were carried out. The FE model was validated by comparing the load–displacement curves of the sandwich panels between experimental and FE analysis, the comparisons show a satisfactory agreement between the experimental and numerical results. Also, analytical Gibson's modified model is considered to obtain the critical loads leading to the failure of the sandwich panels. This allows constructing a mode map for failure modes of sandwich panels in three points bending process.

References

1. Kim KJ, Rhee MH, Bik C (2009) Development of application technique of aluminium sandwich sheet for automotive hood. Int J Precis Eng Manuf 10:71–75
2. Link TM (2001) Formability and performance of steel-plastic-steel laminated sheet materials. In: SAE technical paper, 01-0079
3. Zenkert D, Burman M (2011) Failure mode shifts during constant amplitude fatigue loading of GFRP/foam core sandwich
4. Ferreira JAM, Costa JDM (1998) Static behaviour of PVC foam composite sandwich panel. J Cell Polym 17(3):177–192
5. Gimenez I, Farooq MK, Mahi AEl, Kondratas A, Assarar M (2004) Experimental analysis of mechanical behaviour and damage development mechanisms of PVC foams in static tests. Mater Sci 10(1)
6. Mamalis A, Spentzas K, Manolakos D, Ioannidis M, Papapostolou D (2008) Experimental investigation of the collapse modes and the main crushing characteristics of composite sandwich panels subjected to flexural loading. Int J Crashworthiness 13(4):349–362
7. Andrews EW, Moussa NA (2009) Failure mode maps for composite sandwich panels subjected to air blast loading. Int J Impact Eng 36:418–425
8. Daniel IM, Gdoutos EE, Wang KA, Abot JL (2002) Failure modes of composite sandwich beams. Int J Damage Mech 11:309–334
9. Gdoutos EE, Daniel IM, Wang KA (2003) Compression facing wrinkling of composite sandwich structures. Mech Mater 35:511–522
10. Kim HY, Hwang W (2002) Effect of debonding on natural frequencies and frequency responses functions of honey sandwich beams. Compos Struct 55:51–62 92, 2703–2711
11. Idriss M (2013) Analyse expérimentale et par éléments finis du comportement statique et vibratoire des matériaux composites sandwich sains et endommagés. Thèse de doctorat

12. Gibson LJ, Ashby MF (1997) Cellular solids: structure and properties. Cambridge University Press
13. Allen G (1969) Analysis and design of structural sandwich panels. Pergamon Press, Oxford, p 1969
14. Yu JL, Wang EH, Li JR, Zheng ZJ (2008) Static and low-velocity impact behavior of sandwich beams with closed-cell aluminum-foam core in three-point bending. Int J Impact Eng 35:885–894